Orbital Angular Momentum Detection Using Geometric-phase Based Metasurfaces

Menglin L. N. Chen[1]*, Li Jun Jiang[1], and Wei E. I. Sha[2]

[1]The University of Hong Kong, Hong Kong, China

[2]Zhejiang University, Hangzhou, China

***Contact: menglin@connect.hku.hk**

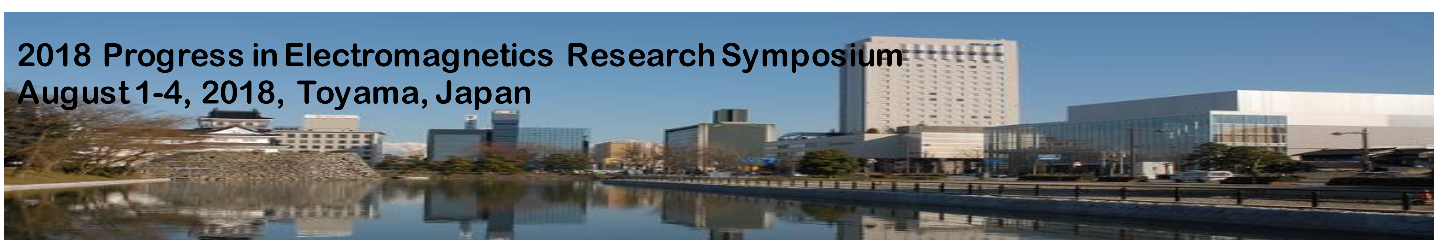

Contents

Introduction

- Orbital Angular Momentum of Light
- Literature Review

Design

- Methodology for Multiple OAM-Beam Detection
- Simulation Results
- Side-Lobe Suppression

Conclusion

- Summary
- Contributions

Angular Momentum

- Spin angular momentum (SAM), value S = 0, ±ħ
- Orbital angular momentum (OAM): value $L = l\hbar$

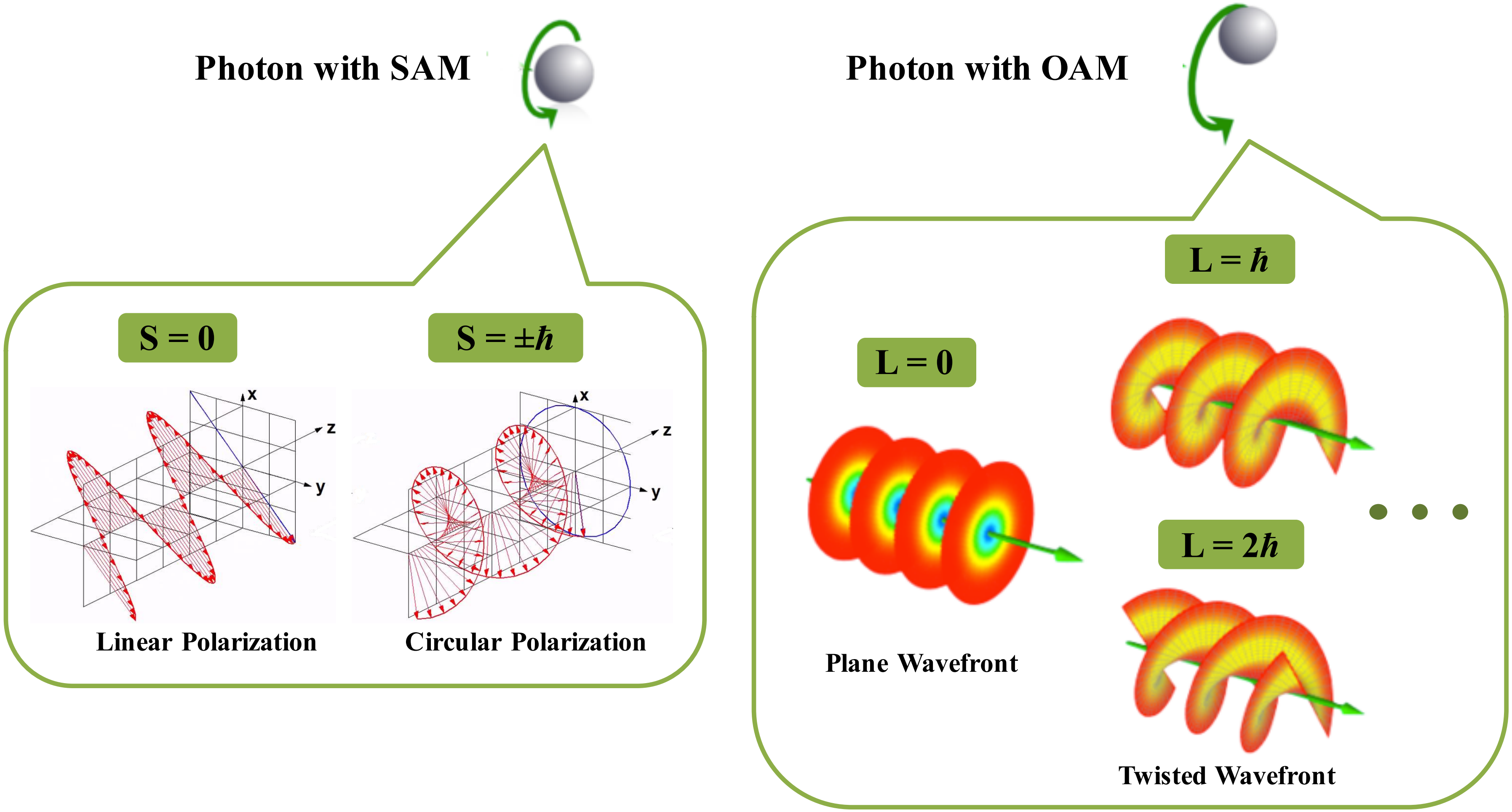

Applications

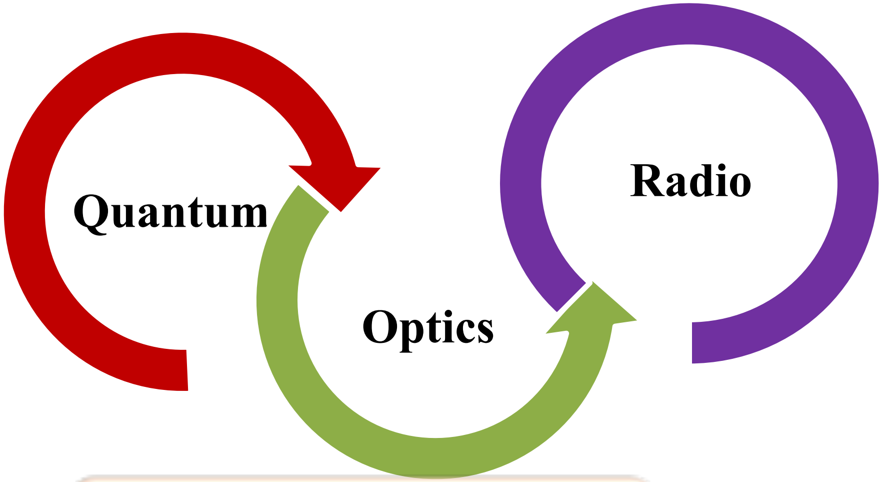

Communications

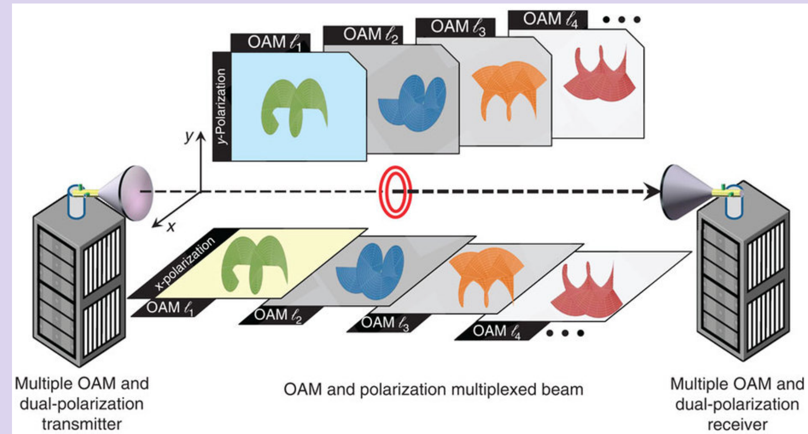

Nat Commun. **5** 4876 (2014)

Quantum Cryptography

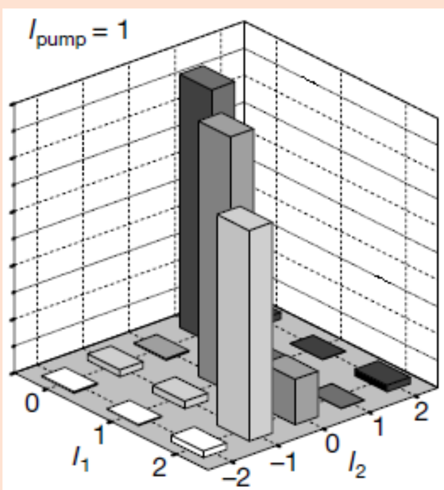

Nature **412** 19 (2001)

Optical Tweezer

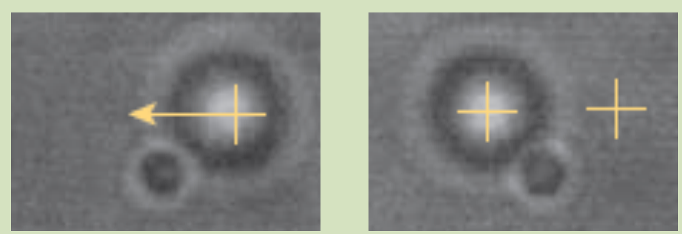

Nature **424** 21 (2003)

Ultrathin Complementary Metasurface

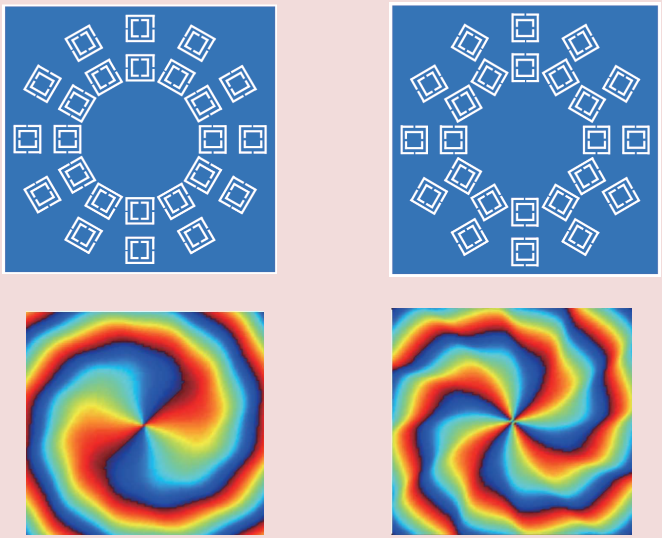

M. Chen, *et al*, IEEE Trans. Antennas Propag., **65** 396 (2017)

Composite PEC-PMC Metasurface

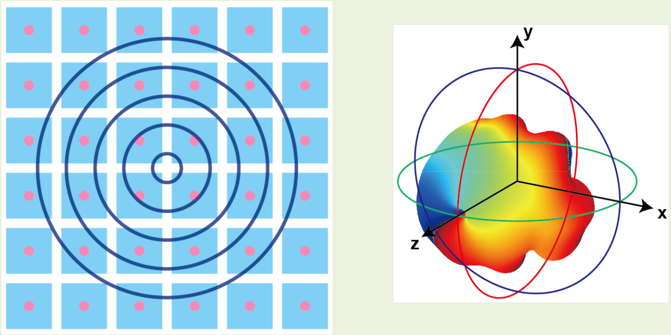

M. Chen, *et al*, *J. Appl. Phys.*, **119** 064506 (2016)

Photonic Crystals

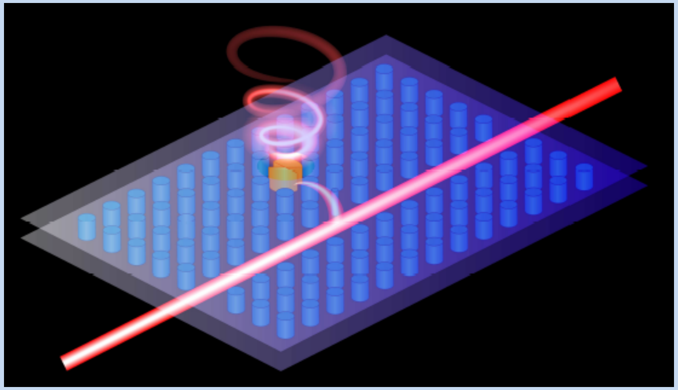

M. Chen, *et al*, *Phys. Rev. Appl.*, accepted.

Literature Review (cont.)

Near-Field Scanning

$$J_z \approx \epsilon_0 \int \mathrm{Re}\{xE_zB_x^* - yE_yB_z^*\}\mathrm{d}V.$$

Radio Sci. **45** RS4007 (2010)

Modal Decomposition

New J. Phys. **15** 073025 (2013)

Local Topological Charge Analysis

Opt. Express **24** 5 (2016)

Holographic Plasmonic Interface

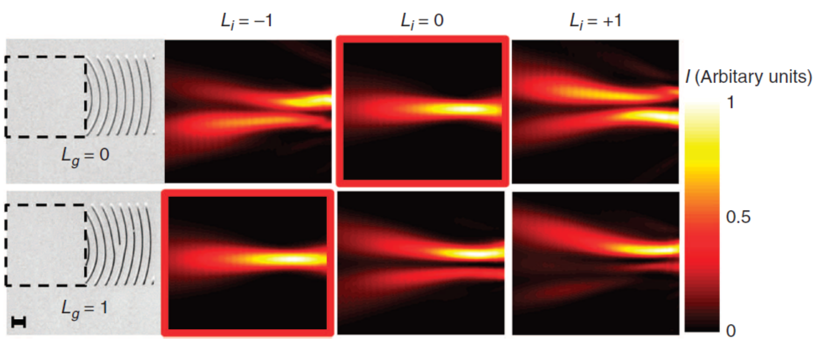

Nat. Commun. **3** 1278 (2012)

Rotational Doppler Shift

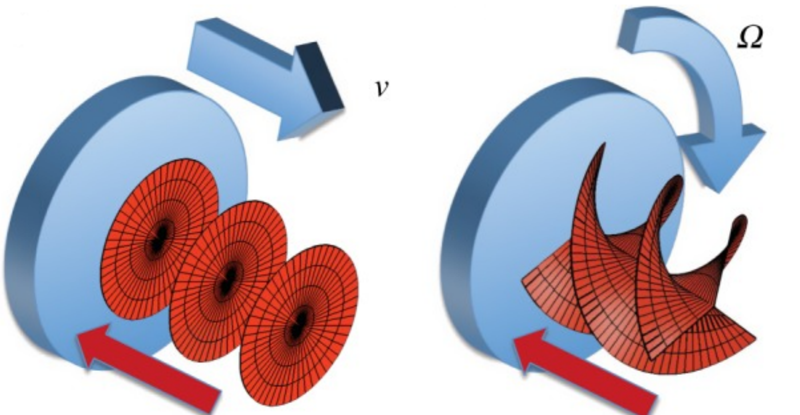

Proc. R. Soc. A **470** 2172 (2014)

Schematic Representation

- **The metasurface converts an OAM beam to a Gaussian beam. The beam axis depends on the order of incident OAM.**
- **By locating the Gaussian beam, the incident OAM can be determined.**

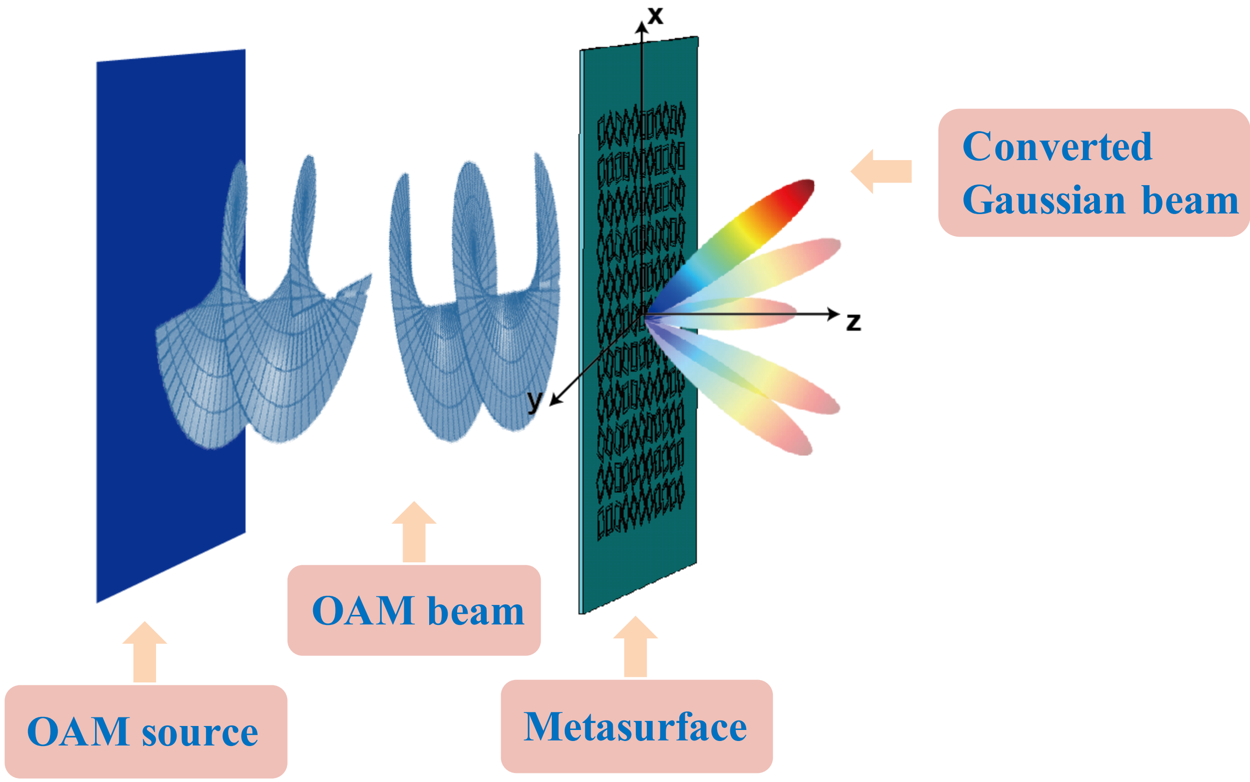

Methodology

➢ Transmission function of an aperture

- ❖ Generation of multiple OAM beams

$$t(r,\phi)=\sum_m A_m e^{j(l_m\phi+k_{xm}x+k_{ym}y)}$$

r is the radial position, φ is the azimuthal position, A_m is the weight of the m^{th} beam, l_{m} is the corresponding OAM index, and k_{xm}, k_{ym} are the transverse wave numbers of the m^{th} beam.

➢ Far-field response

- ❖ Fourier transform

$$E=F\{E_{\text{in}}\cdot t\}$$

➢ Example

- ❖ Five-beam generation: $l_1 = 2$, $l_2 = 1$, $l_3 = 0$, $l_4 = -1$, $l_5 = -2$
- ❖ At the directions of $\theta = 40°$ and $\varphi = 90°$, $18°$, $306°$, $234°$, $162°$ ($k_{x1\sim5}$, $k_{y1\sim5}$)
- ❖ Plane wave incidence

Each beam has same power

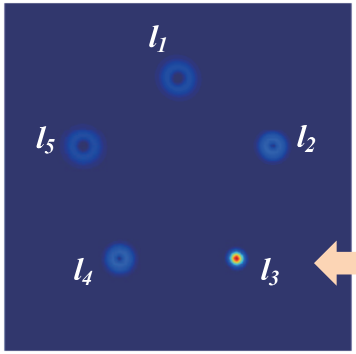

Detectable

Methodology (cont.)

- **Under the incidence of Laguerre-Gaussian Beam (LG_{0l_0})**

$$\boxed{E_{\text{in}}(r,\phi) = r^{l_0} e^{-r^2/w^2} e^{jl_0\phi}}$$

w is the beam waist.

- **Far-field response**
  - At the k-space position (k_{xm}, k_{ym}), the OAM order is $l_m + l_0$.

$$\boxed{E = F\{E_{\text{in}} \cdot t\} = \sum_m A_m F\{E_{\text{OAM}(l_m+l_0)}(k_{xm}, k_{ym})\}}$$

- **Detection process**

Measure beam intensity at (k_{xm}, k_{ym}) → **Detect the Gaussian beam (k_{xM}, k_{yM})** → **$l_0 = - l_M$**

Aperture Implementation

➢ **Geometric-phase metasurface**

❖ Phase of transmission function is extracted: $\arg(t(r,\phi))$

❖ Phase profile is reconstructed using complementary split ring resonators (CSRRs)

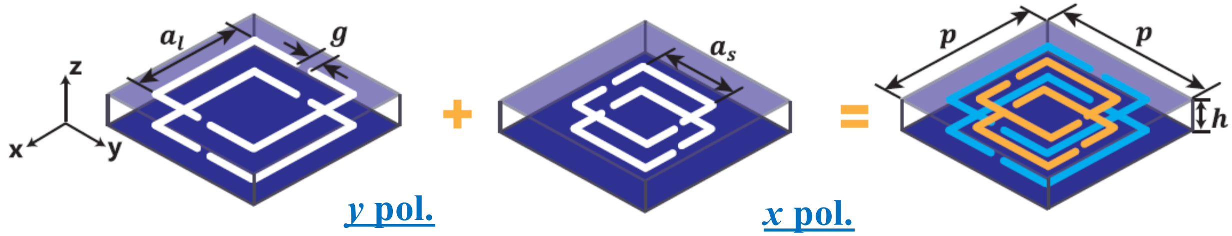

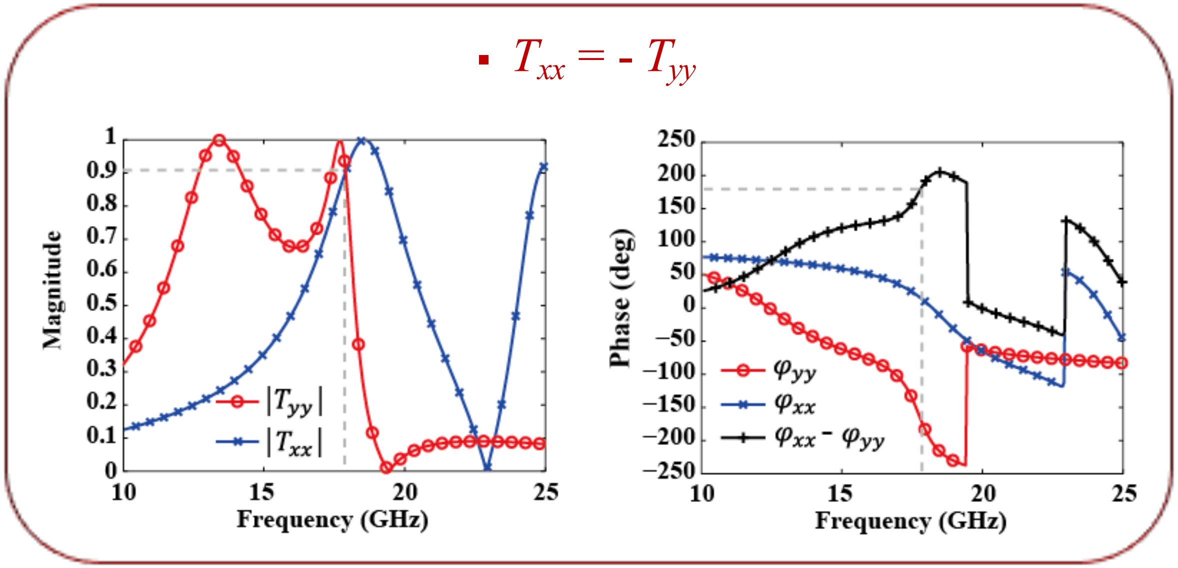

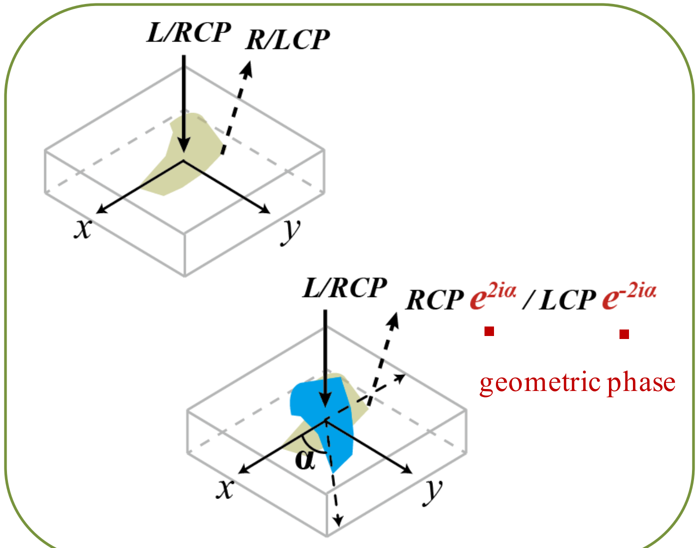

Aperture Implementation (cont.)

- **Geometric-phase metasurface**
  - Phase profile is discretized by 11 × 11 pixels
  - Each pixel is implemented using CSRRs
- **Simulation approaches**
  - Full-wave simulations, CST MWS
  - Equivalent magnetic dipoles

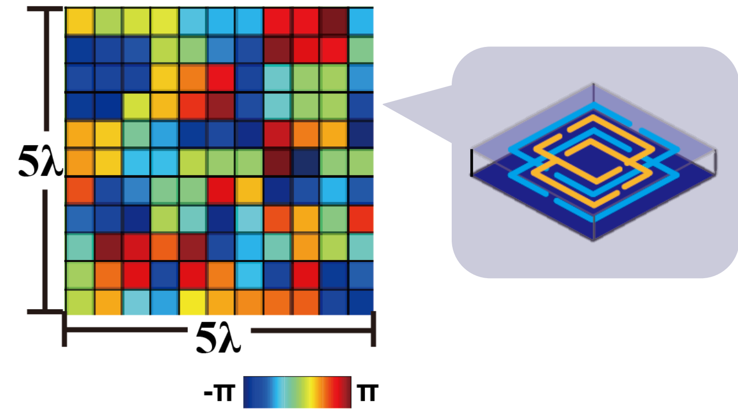

Top view of the metasurface

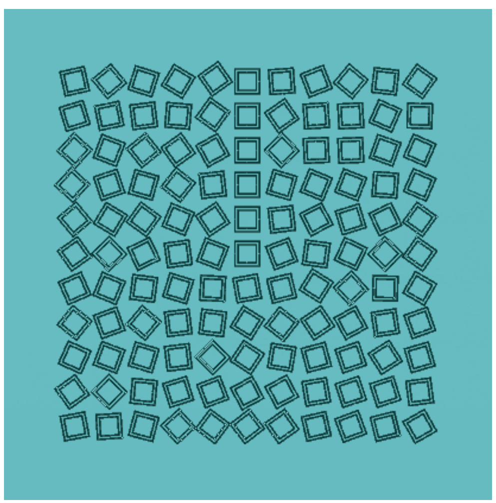

- Response of the metasurface is equivalent to that of magnetics dipoles at different locations with different orientations

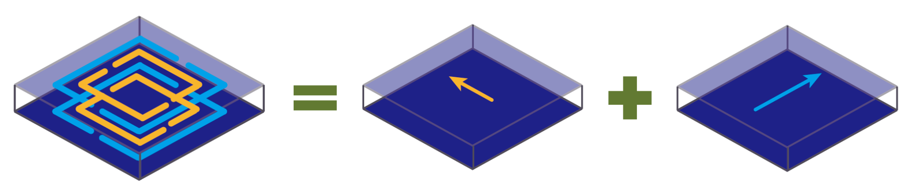

$$\mathbf{E}(\mathbf{r}) = 2\int_V \overline{\mathbf{G}}_m(\mathbf{r},\mathbf{r}')\cdot\mathbf{M}(\mathbf{r}')d\mathbf{r}' = 2\int_V \nabla g(\mathbf{r},\mathbf{r}')\times\mathbf{M}(\mathbf{r}')d\mathbf{r}'$$

- Comparison between the simulation results using equivalent dipole model and commercial software

Incident beam	$LG_{0,-2}$, $l = -2$	$LG_{0,-1}$, $l = -1$	$LG_{0,0}$, $l = 0$	$LG_{0,1}$, $l = 1$	$LG_{0,2}$, $l = 2$
Equivalent dipoles 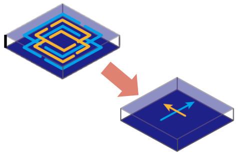	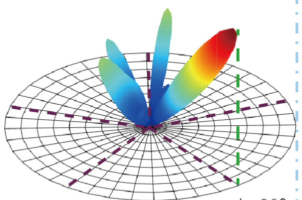	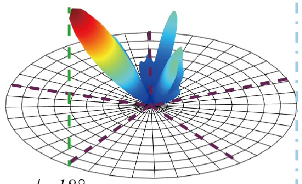	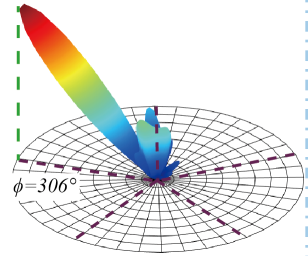	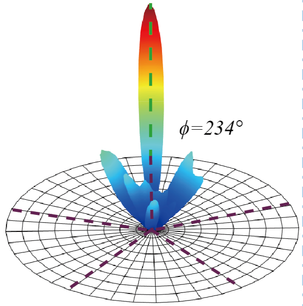	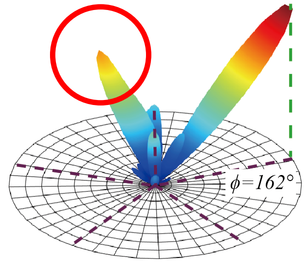
CST MWS				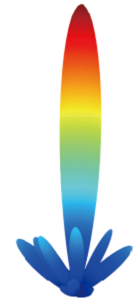	

Side-Lobe Suppression

- **Reason for high side lobe**
  - Constructive interference among multiple beams, especially between two adjacent beams

- **Modified transmittance function**

$$t_{\text{mod}}(r, \phi) = \sum_{m} e^{j(l_m \phi + k_{xm} x + k_{ym} y + \underline{\alpha_m})}$$

- **Example**
  - The beam with *l=1* is rotated by -90°.
  - The rotation changes the phase of the beam at the previous interference area, resulting in a weakened field intensity.

Original: $\alpha_{1,2,3,4,5} = 0$ **Modified: $\alpha_{1,3,4,5} = 0, \alpha_2 = -1.5708$**

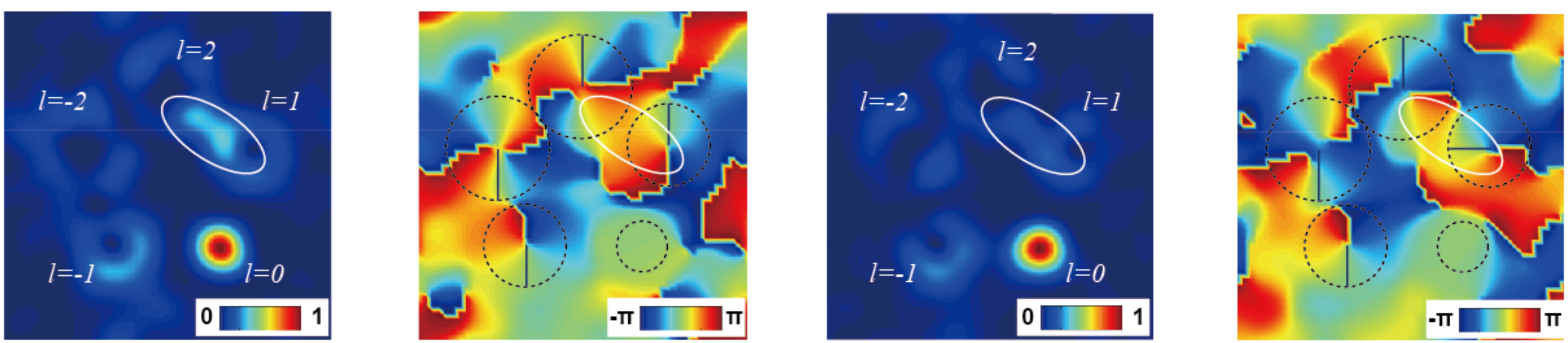

Optimized Results

- **Optimization objective**
  - Maximizing the minimum peak-to-sidelobe ratio
- **Optimal solution**
  - $\alpha_1 = 1.0472, \alpha_2 = 1.0472, \alpha_3 = 2.0944, \alpha_4 = 2.7925, \alpha_5 = 4.5379$
- **Comparison results**
  - Field intensity along the azimuthal coordinate is plotted at $\theta = 40^{\circ}$.
  - Overall, we can observe suppressed side lobes and increased field intensities at desired locations.

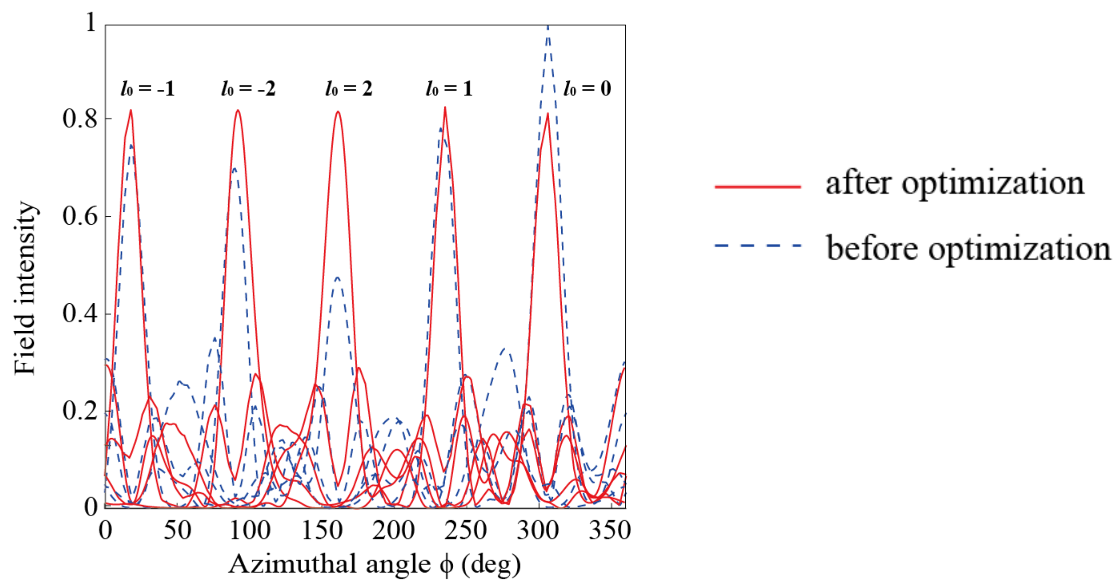

Conclusions

- ✓ **Orbital angular momentum (OAM), $L = l\hbar$**
- ✓ **An innovative OAM-detection approach is proposed**
  - The OAM wave is converted to a zero-OAM wave whose directivity depends on the incident OAM order.
  - A metasurface that can detect five OAM orders is implemented using CSRRs.

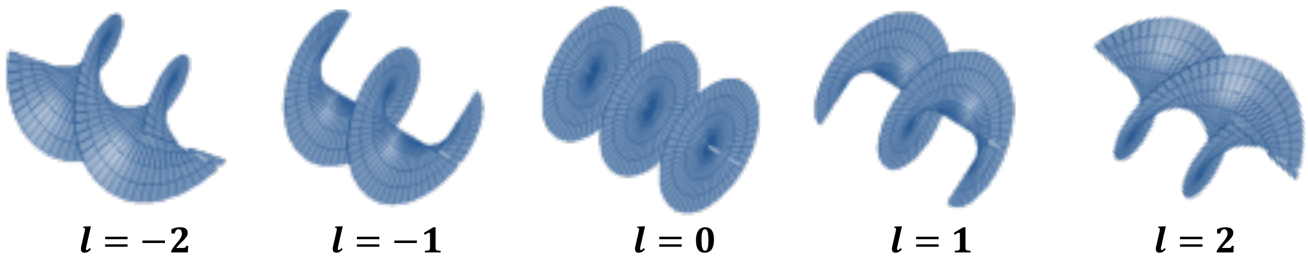

  - A novel modified transmission function is proposed to optimize the metasurface.

Reference:

1. **M. L.N. Chen**, L. J. Jiang, and W. E.I. Sha, "Orbital Angular Momentum Generation and Detection by Geometric-Phase based Metasurfaces", *Appl. Sci.*, vol. 8, pp. 362, Mar. 2018.
2. **M. L.N. Chen**, W. E.I. Sha, and L. J. Jiang, "Detection of Orbital Angular Momentum with Metasurface at Microwave Band", *IEEE Antennas Wireless Propag. Lett.*, vol. 17, no. 1, pp. 110–113, Jan. 2018.
3. **M. L.N. Chen**, L. J. Jiang, and W. E.I. Sha, "Ultrathin Complementary Metasurface for Orbital Angular Momentum Generation at Microwave Frequencies", *IEEE Trans. Antennas Propag.*, vol. 65, no. 1, pp. 396–400, Jan. 2017.
4. **M. L.N. Chen**, L. J. Jiang, and W. E.I. Sha, "Artificial Perfect Electric Conductor-Perfect Magnetic Conductor Anisotropic Metasurface for Generating Orbital Angular Momentum of Microwave with Nearly Perfect Conversion Efficiency", *J. Appl. Phys.*, vol. 119, no. 6, pp. 064506, Feb. 2016.

Thanks for your attention!

Contact: menglin@connect.hku.hk